Available online at www.sciencedirect.com

ScienceDirect

Procedia Engineering 102 (2015) 527 – 533

Procedia Engineering

www.elsevier.com/locate/procedia

The 7th World Congress on Particle Technology (WCPT7)

Size dependent heating efficiency of iron oxide single domain nanoparticles

Harshida Parmar[a*], Ilona S. Smolkova[a], Natalia E. Kazantseva[a], Vladimir Babayan[a], Petr Smolka[a], Robert Moučka[a], Jarmila Vilcakova[a], Petr Saha[a]

[a]*Centre of Polymer Systems, University Institute, Tomas Bata University in Zlin, 760 01 Zlin, Czech Republic*

Abstract

The iron oxide nanoparticles have been synthesized by coprecipitation and solvothermal reduction methods. The particles obtained differ in size, the mean size of particles coprecipitated is of 13nm and the particles, prepared by solvothermal reduction method have a size of 20nm. Both kinds of nanoparticles demonstrate narrow particles sizes distribution. The particles which are prepared by coprecipitation method have narrow particles sizes distribution with mean size diameter of 13nm and the particles, prepared by solvothermal reduction method have a size of 20nm. The X-ray diffraction data analysis revealed that highly crystalline and single-phase magnetite nanoparticles are formed by solvothermal reduction technique, whereas coprecipitation leads to the formation of multi-phase composition of a magnetite (72%) and maghemite (28 %). According to the size of nanoparticles obtained, they are in superparamagnetic state for iron oxides. The saturation magnetization of solvothermal prepared particles is higher than those for coprecipitated due to their higher crystallinity and phase purity. Nevertheless, the glycerol dispersion of particles coprecipitated shows higher SLP values than the dispersion of the particles, synthesized by solvothermal reduction method. The heating efficiency of nanoparticles based dispersions is explained by the particles size effect and properties of carrier medium.

Selection and peer-review under responsibility of Chinese Society of Particuology, Institute of Process Engineering, Chinese Academy of Sciences (CAS)

Keywords: Iron oxide nanoparticles; Hyperthermia; Specific loss power; monodisperse nanoparticles

* Corresponding author. +420 576 038 151; fax: +420 576 031 444.
E-mail address: harshidag@gmail.com (Harshida Parmar).

Selection and peer-review under responsibility of Chinese Society of Particuology, Institute of Process Engineering, Chinese Academy of Sciences (CAS)
doi:10.1016/j.proeng.2015.01.205

1. Introduction

A wide range of ferromagnetic nanoparticles (NPs), including metals/alloys with superior magnetic properties, can be synthesized for magnetic mediated hyperthermia (MMH)[1,2]. Among the nanoparticles that can be used for MMH are iron oxides, namely magnetite (Fe_3O_4) and maghemite (γ-Fe_2O_3) due to their high magnetization, low biocompatibility and their known pathways of metabolism[3]. However, there are other properties, such as high absorption in the tumor cells, which the nanoparticles must possess in order to be used in this method. The size of nanoparticles determines to a large extend their suitability for the method *in vivo*. The efficiency of MMH is characterized by the specific loss power (SLP) at certain frequency and strength of magnetic field. To use MMH in clinical practice, a first challenge is to developed a mediator (NPs in carrier medium) with high SLP at frequency (f) and intensities (H) of an AC magnetic field that allowed for medical application ($H \leq 15$ kA.m^{-1} ; $0.05 \leq f \leq 1.5$ MHz)[4].

It is well known that magnetite and maghemite can be prepared by many synthesis rotes. The formation of product by organic methods, like thermal decomposition, requires a few hours. In contrast, aqueous methods like coprecipitation of iron salts are more simple and economic. The heating potential of magnetic NPs, which is estimated by SLP, strongly depends on the set of parameters: (1) morphology (particle shape, size, size distribution, (2) structure (crystallinity, phase formation), (3) magnetic properties (anisotropy constant, saturation magnetization, coercive force, *etc*). These parameters depend on the nanoparticles synthesis procedure and preparation conditions. For hyperthermia treatment, particles with size around the superparamagnetic - stable single domain transition have been found to have the maximum SLP values[5,6].

2. Experimental part

Nanoparticles were synthesized by two chemical methods – co-precipitation (sample I) of iron (II) and iron (III) chlorides and solvothermal method by modified reduction reaction between $FeCl_3$ and ethylene glycol (sample II). In co-precipitation reaction ferrous and ferric chlorides (both are hydrates) in a molar ratio 1:2 were utilized. Two solutions were prepared – ammonia hydroxide solution as a source of OH- ions and a solution of iron chlorides. The basic solution was heated to 70^o C and kept under constant continuous mechanical stirring and argon purging. When the desired temperature is gained, iron salts solution was added under control rate to the ammonia solution and the reaction started immediately – a color of media became black and a bit brownish. The nucleation occurred as first drops of iron salts reached the ammonium solution. The black powders of iron oxide nanoparticles formed in the reaction were separated by a permanent magnet, washed with distilled water to neutral pH and dried in air at room temperature.

Sample II was synthesized using solvothermal reduction method. It is known that solvothermal reduction method is used to synthesize monodispersed particles. $FeCl_3 \cdot 6H_2O$ (2.7 g, 10 mmol) was dissolved in ethylene glycol (120 mL) to form a solution, followed by the addition of NaAc (12 g) and polyethylene glycol (2 g). The mixture was stirred vigorously for 30 min and then heated to 200^{o}C for 19 h. At the end of the synthesis the reaction media was allowed to cool down to room temperature. The black products were washed several times with ethanol and dried at room temperature.

Sample II was characterized on a PANalytical X-Ray powder diffractometer equipped with PIXcel RTMS detector with CuKα radiation (λ=1.5418Å) and sample I was characterized using X'pert Pro MPD with MoKα radition (λ=0.7107Å). The X-Ray diffraction (XRD) data are refined by Rietveld refinement technique using Fullprof program. The average crystallite size is determined using Scherrer's formula (incorporated in Rietveld refinement) given by $Dx = 0.89\lambda/B \cos\theta$, where Dx is the mean crystallite diameter of the particle, λ is the wavelength of radiation of the x-ray, θ is the diffraction peak angle, and B is the line width at observed half-peak intensity.

The amount of PEG coating the iron oxide nanoparticles was determined by thermogravimetric analysis (TGA) using a TGA Q500 (TA Instruments) with a 10 ◦C/min heating rate under nitrogen atmosphere (10 mL min−1). The measurement was made from room temperature up to 500 ◦C.

The magnetization measurements were performed with a Vibrating Sample Magnetometer (Lake Shore 7404) at room temperature in air atmosphere in magnetic field of up to 10 kOe. The amplitude and the frequency of vibration were 1.5 mm and 82 Hz, respectively. The samples were measured in the form of powders.

The thermal response of iron oxide nanoparticles in an AC magnetic field was studied using calorimetric measurements. The measuring system consisted of an oscillator (Tektronix AF6 3021B), power amplifier (AR worldwide Model 800A3), induction coil, interchangeable capacitors and measuring units for temperature and magnetic field sensing. The measurements were carried out at an AC magnetic field frequencies of 114, 525, 1048 kHz and intensities of 5.9, 7.6, 13.8 kA·m^{-1}. The test tube with a sample in the form of a dispersion of iron oxide magnetic nanoparticles (5 wt. %) in glycerol was inserted into a solenoid coil with an AC magnetic field. The glycerol dispersions of nanoparticles were prepared with ultrasonic homogenizer Sonoplus HD 2070. Both samples were temperated at 25 °C in a water bath before each measurement. The temperature was measured with optical hot spot module (Qualitrol TGL 589A) and fiber optic temperature sensor (T1S-03_PT06) inserted directly inside the sample dispersions.

The SLP was calculated as follows [7,8]:

$$SLP = \frac{1}{m}\left[\left(\frac{dT}{dt}\right) \cdot C\right],$$

where m is the mass of the iron oxide nanoparticles in the glycerol dispersion; $\frac{dT}{dt}$ is the slope of temperature rise in time curve; and C [J·K^{-1}] is the heat capacity of a sample in the form of the dispersion consisting of n components,

$$C = \sum_{i=1}^{n} x_i m_i,$$

where x_i [J·g^{-1}·K^{-1}] is the specific heat capacity of a component and m_i [g] is the mass a component of the sample. The following values were used in the calculations: x *(glycerol)* = 2.434 J·g^{-1}·K^{-1}; x *(magnetite)* = 0.5 J·g^{-1}·K^{-1}. Because the experimental set-up is not perfectly adiabatic, the $\frac{dT}{dt}$ value was determined from the initial slope of temperature increase obtained from the linear term of polynomial fit of the whole curve.

3. Result and discussion

3.1. Structural properties of iron oxides

The XRD pattern of both samples exhibits 9 lattice planes (111), (220), (311), (222), (400), (422), (511), (440), (531) corresponding to the cubic spinel structure of magnetite phase. In sample I the two remarkable lattice planes (210) and (213) corresponding to the tetragonal structure of maghemite phase (Figure 1). The XRD data refinement has been done using Fd3m space group for magnetite phase and $P4_12_12$ space group for maghemite phase. It is established that Sample I comprises of 72% of magnetite and 28 % of maghemite phase, whereas Sample II contains of pure magnetite. This mixed phase composition of nanoparticles is consistent with previously reported result for iron oxide nanoparticles obtained by coprecipitation method[9,10].

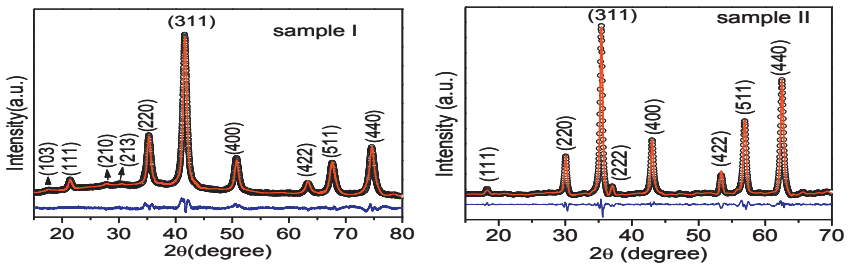

Fig. 1. XRD pattern of Sample I and II. The points are the observed data, and continuous line is the calculated pattern using Fullprof program Reitveld refinement technique.

The calculated crystalline size from the XRD data for sample I and II are 13nm and 20nm respectively. It is known that magnetite particles below a size threshold of 20 – 30 nm are SPM, and above this threshold (approximately up to 50 – 80nm) they are in a stable SD state (ferromagnetic regime); with the size increase above 80 – 100 nm, particles are multidomain[11]. Therefore, according to the particle sizes calculated from XRD, sample I is in SPM state, while Sample II is on the transition edge from SPM to SD state (probably in pseudo-single domain state). Structural parameters obtained from the Reitveld refinement of XRD pattern are listed in Table 1.

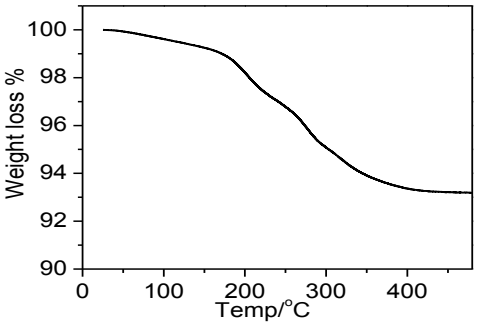

Fig. 2. Weight loss of magnetic particles coated with PEG determined from Thermal Gravimetric Analysis (TGA)

The TGA curve (Figure 2) shows a slight loss of weight ranging of 1.53% in the temperature range of 30–160 °C due to the moisture content in the sample. The mass profile exhibited a well defined decrease over a temperature range of 160–450°C. This weight loss is due to the desorption and subsequent evaporation of PEG from the surface of particle. However, this weight loss is only about 6% thus the coverage of particle surface by the polymer is not complete. In this way, particles can magnetically interact and form aggregates[12]

Table 1: Different synthesis method effect on structural parameters determined from XRD pattern analysis

sample	*a* ± 0.0004, (Å)		d_{XRD} ± 0.8, (nm)	Magnetite content ± 3%	Maghemite content ± 3%	R_F	R_{Braga}	R_F	R_{Braga}
	Magnetite	Maghemite				Magnetite		Maghemite	
I	8.3584	a=b=8.3466 c=25.0189	13	72	28	2.6	3.4	4.1	5.9
II	8.3947	-	20	100	-				

3.2. Magnetic properties of iron oxides

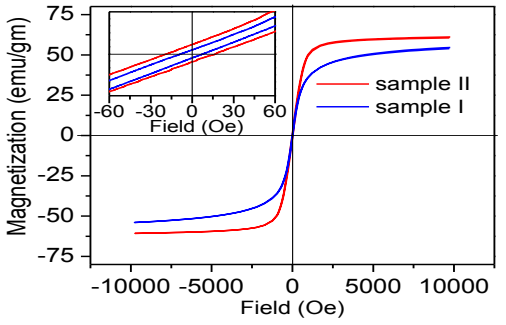

Fig. 3. The Magnetization curves for Sample 1 and Sample II. Insets: (a) magnetization at low magnetic fields

The room temperature magnetization curve is shown in Figure 3. The Sample I show the non saturating behavior even at field of 10kOe whereas sample II reached to the saturation at the field of 6kOe. The magnetic parameters like M_S, M_R and H_C for Sample II and I are 62 emu/g, 2 emu/g, 18 Oe and 57 emu/g, 8 Oe respectively. Sample II has higher values of all magnetic parameters than that of Sample I (M_S=57 emu/g) due to higher crystallinity and phase purity that those for sample I. The value of M_S for both samples is lower than that for bulk magnetite due to the size effect caused by strong disorder of spins on the surface. Magnetization curve of Sample II indicates its ferromagnetic behavior: sample is saturated state and demonstrates remarkable coercivity and remanence magnetization. On the contrary, Sample I is not saturated even in the magnetic field of 10 kOe and characterized by low coercivity and almost zero remanence magnetization which indicates the higher surface anisotropy in the sample I than sample II.

3.3. Heating efficiency of iron oxide NPs dispersed in a viscous medium

Figure 4 shows the temperature evolution curves for both samples at different AC magnetic field parameters. The thermal response depends on many parameters like particle size, size distribution, interparticle interactions, dosage of particles in carrier medium and its viscosity and heat capacity, and moreover effect of nanoparticles surface modification. As it is known, mainly two magnetic relaxations contribute to the magnetic loss in ensemble of nanoparticles in AC magnetic field, i.e. internal relaxation (Neel) and external relaxation (Brownian). Internal relaxation of the magnetic moment inside the nanocrystal originates from magnetic anisotropy energy which tends to orient the magnetic moment in specific directions called easy axes (Neel mechanism). External relaxation is due to the viscosity of the carrier fluid, impeding thermal fluctuations of the particle itself (Brownian mechanism). Characteristic times of Neel (internal) and Brownian (external) relaxations (in comparison with the magnetic field frequency) determine the heating power of the nanoparticles. Both mechanisms depend on particle size, whereas only the Brownian contribution depends on viscosity and only the Neel contribution is tuned by the magnetic anisotropy of the material. The heating efficiency of nanoparticles in the current work was investigated on the glycerol dispersions providing the elimination of the Brownian relaxation contribution to the magnetic losses in AC magnetic field due to high viscosity of the dispersion media[13]. This particular condition is taking place when the nanoparticles are administered into the tumor tissue[14]. The calculated values of SLP are listed in Table 2. According to the results obtained, sample I shows the temperature increases from 37 ^{0}C to the hyperthermia temperatures (42^{0}C – 45^{0}C) in tens of seconds, furthermore the value of SLP increases with frequency and the field intensity. Contrariwise, sample II shows a very low heating rate.

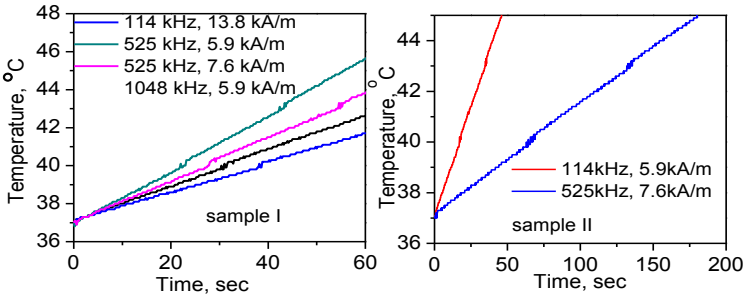

Fig. 4. Heating rate of the Sample I and Sample II dispersed in glycerol (5 wt. % of nanoparticles) for given frequency and amplitude of AC magnetic field

The heating characteristics of particles are a complex function of the properties of individual nanoparticles and their collective magnetic behaviour. It was showed that the effect of inter-particles interactions on SLP is still not completely understood. The experimental studies reveal as increase[15,16] as decrease[17] of SLP with interactions. The primary mechanism leading to the variation of SLP in magnetically interacting particles is a variation of energy

barrier[18]. The high heating potential of Sample I is determined by narrow particle size distribution and inter-particles interactions which change the nature of the SPM to being thermally stable (SPM – stable SD transition).

Table 2: Specific loss power of Sample I and Sample II dispersed in glycerol (5 wt. % of nanoparticles)

AC magnetic field		SLP, $W.gm^{-1}$	
Frequency, kHz	Amplitude, $kA{\cdot}m^{-1}$	Sample I	Sample II
114	13.8	13.3	10.1
525	5.9	9.4	-
	7.6	16.8	2.3
1048	5.9	16.4	-

As of particle size of sample I (13nm), is smaller than the sample II (20nm). For small size nanoparticles the Neel relaxation time (internal relaxation of magnetic moment in the particle) is much higher than the Brownian relaxation time (external relaxation of magnetic moment by the rotation of particle), and on further growth of size follows closely the Brownian relaxation[19]. The critical diameter for transition from Neel relaxation to Brownian relaxation depends on particle size and effective value of magnetic anisotropy. It seems that low heating rate of Sample II connected with high value of magnetic anisotropy which limits the Neel relaxation. At the same time, the high viscosity of glycerol prevents the Brownian relaxation.

4. Conclusion

Iron oxide magnetic nanoparticles have been obtained by coprecipitation and solvothermal reduction methods. The X-ray diffraction analysis revealed that the sample II has a pure single phase magnetite phase while sample I exhibit the mixture of 72 % magnetite and 28% maghemite phases. Despite the high values of M_S, H_C for Sample II, its dispersion in glycerol shows significantly lower SLP values than those for sample I. The low value of SLP for sample II can be explained by high value of magnetic anisotropy which limits the contribution of Neel relaxation and by high viscosity of glycerol which prevents contribution from Brownian relaxation.

Acknowledgements

This work was produced with support of Operational Program Education for Competitiveness co-funded by the European Social Fund (ESF) and national budget of Czech Republic, within the framework of project Advanced Theoretical and Experimental Studies of Polymer Systems (reg. number: CZ.1.07/2.3.00/20.0104) as well as with the support of Operational Program Research and Development for Innovations co-funded by the European Regional Development Fund (ERDF) and the National budget of Czech Republic, within the framework of project Centre of Polymer Systems (reg. number: CZ.1.05/2.1.00/03.0111)

References

[1] S. Sun, C.B. Murray, Synthesis of monodisperse cobalt nanocrystals and their assembly into magnetic superlattices, J. Appl. Phys. 85(1999) 4325–4330.

[2] S. Sun, Recent Advances in Chemical Synthesis, Self-Assembly, and Applications of FePt Nanoparticles, Adv. Mater. 18(2006) 393–403

[3] M. Gonzales, L.M. Mitsumori, J.V. Kushleika, M.E. Rosenfeld, K.M. Krishnan, Cytotoxicity of iron oxide nanoparticles made from the thermal decomposition of organometallics and aqueous phase transfer with Pluronic F127, *Contrast Media and Molecular Imaging 5(*2010) 286–293

[4] P. Hanggi, P. Talkner, M. Borkovec, Reaction-Rate Theory - 50 Years after Kramers, Rev. Mod. Phys. 62(1990) 251-341

[5] A. Jordan, R. Scholz, P. Wust, H. Fahling, R. Felix, Magnetic fluid hyperthermia (MFH): Cancer treatment with AC magnetic field induced excitation of biocompatible superparamagnetic nanoparticles, J. Magn. Magn. Mater. 201(1999) 413-419

[6] M. Andres-Verges, R. Costo, A. G. Roca, J. F. Marco, G. F. Goya, C. J. Serna, M. P. Morales, Uniform and water stable magnetite nanoparticles with diameters around the monodomain–multidomain limit, J. Phys. D: Appl. Phys. 41(2008) 134003-22

[7] A. Jordan, P. Wust, H. Fahling, W. John, A. Hinz, R. Felix, Inductive heating of ferrimagnetic particles and magnetic fluids: Physical evaluation of their potential for hyperthermia, Int. J. Hyperther. 25(2009) 499-511
[8] S. Laurent, S. Dutz, U.O. Hafeli, M. Mahmoudi, Magnetic fluid hyperthermia: focus on superparamagnetic iron oxide nanoparticles,Adv. Colloid Interfac. 166(2011) 8-23.
[9] J. Murbe, A. Rechtenbach, J. Topfer, Synthesis and physical characterization of magnetite nanoparticles for biomedical applications, Mater. Chem. Phys. 110(2008) 426-433
[10] R.L. Rebodos, P.J. Vikesland, Effects of oxidation on the magnetization of nanoparticulate magnetite, Langmuir 26(2010) 16745-16753
[11] J. Baumgartner, L. Bertinetti, M. Widdrat, A.M. Hirt, D. Faivre, Formation of Magnetite Nanoparticles at Low Temperature: From Superparamagnetic to Stable Single Domain Particles, Plos One, 8(2013) e57070
[12] Sonia García-Jimeno, Joan Estelrich, Ferrofluid based on polyethylene glycol-coated iron oxide nanoparticles: Characterization and properties, Colloids and Surfaces A: Physicochem. Eng. Aspects 420(2013) 74-81
[13] Y.L. Raikher, V.I. Stepanov, Physical aspects of magnetic hyperthermia: Low-frequency ac field absorption in a magnetic colloid, *J. Magn. Magn. Mater.* 368(2014) 421–427
[14] S. Dutz, R. Hergt, Magnetic nanoparticle heating and heat transfer on a microscale: Basic principles realities and physical limitations of hyperthermia for tumour therapy, Int J Hyperthermia 29(2013) 790-800
[15] L. Lartigue, P. Hugounenq, D. Alloyeau, S.P. Clarke, M. Levy, J.C. Bacri, R. Bazzi, D.F. Brougham, C. Wilhelm, F. Gazeau, Cooperative Organization in Iron Oxide Multi-Core Nanoparticles Potentiates Their Efficiency as Heating Mediators and MRI Contrast Agents, Acs Nano, 6(2012) 10935-10949.
[16] D.E. Bordelon, C. Cornejo, C. Gruttner, F. Westphal, T.L. DeWeese, R. Ivkov, Magnetic nanoparticle heating efficiency reveals magneto-structural differences when characterized with a wide ranging and high amplitude alternating magnetic field., J Appl Phys 109(2011) 124904.
[17] A. Urtizberea, E. Natividad, A. Arizaga, M. Castro, A. Mediano, Specific absorption rates and magnetic properties of ferrofluids with interaction effects at low concentrations, J Phys Chem C, 114(2010) 4916-4922
[18] J.L. Dormann, F. D'Orazio, F. Lucari, E. Tronc, P. Prene, J.P. Jolivet, D. Fiorani, R. Cherkaoui, M. Nogues, Thermal variation of the relaxation time of the magnetic moment of gamma -Fe2O3 nanoparticles with interparticle interactions of various strengths, Phys Rev B Condens Matter 53(1996) 14291-14297
[19] Odenbach S 2003 Magnetoviscous Effects in Ferrofluids (Springer Lecture Notes in Physics) (Heidelberg: Springer)